# IMU-based Active Safe Control of a Variable Stiffness Soft Actuator

Nan Lin[1], Peichen Wu[1], Menghao Wang[2], Jizhou Wei[3], Fan Yang[2], Songlin Xu[3], Zhicheng Ye[3] and Xiaoping Chen[1]

***Abstract*—Using soft pneumatic actuators is a feasible solution in the dynamic unstructed environment, thanks to their light weight and inherent compliance. It is commonly agreed that the passive compliance and adaptivity of soft robots make them much safer. However, under some special circumstances where stringent safety is requested (e.g., surgical operation), the passive compliance is far from meeting the demands. Therefore, active compliance control is still required to guarantee their operating safety.**

**In this paper, a novel soft actuator is presented, whose stiffness is tunable in multiple ways, and more than a 10-fold stiffness enhancement is achievable, making it able to carry heavy loads while maintaining excellent dexterity and compliance. Meanwhile, we first proposed an active safe control strategy based on inertial measurement units (IMUs). Through calibrating the load weight (i.e., weight of the end tools) and measuring vibration of soft structures, the collision can be detected in real-time and the corresponding safe reaction is then adopted. We have validated its effectiveness on human body, the strategy still works at the speed of 200 mm/s with sharp tools. Furthermore, our control strategy can be applied to other soft or continuum robots, making them safer and more practical in actual applications.**

***Index Terms*—Soft robot materials and design, soft sensors and actuators, robot safety.**

## I. INTRODUCTION

SOFT-BODIED robots, which are based on compliant materials and structures, has become an emerging research field, gaining interest in the robotics community [1]. Traditional actuators, like electric motor and air cylinder, play an important role in industrial manufacture, because they can generate rapid and precise motions, making them excel at repetitive tasks in structured environments. But from the perspective of most soft robot researchers, soft robots can adapt to the environment better than rigid-bodied robots [2], [3], therefore they have fewer potential safety threats in human-robot interactions. However, this viewpoint is somewhat one-sided. Up to now some advanced collaborative robots, by precisely measuring the joint torques and establishing accurate impact models [4], even the soft-tissue injury model [5], can detect the impacts in real time, and then take collision reaction strategies correspondingly. But for soft robots, the stringent safety is hard to be guaranteed only by its passive compliance and adaptivity in dangerous human-robot interactions like surgical operation. Besides, most current researches on soft robots are still focusing on kinematics problems [6], [7], and there is no widely accepted dynamic model for safe control, so it's more practical for soft robots to adopt active compliance control in order to guarantee the safety of robot-environment interactions. Unfortunately, few researches focus on this field in soft robotics.

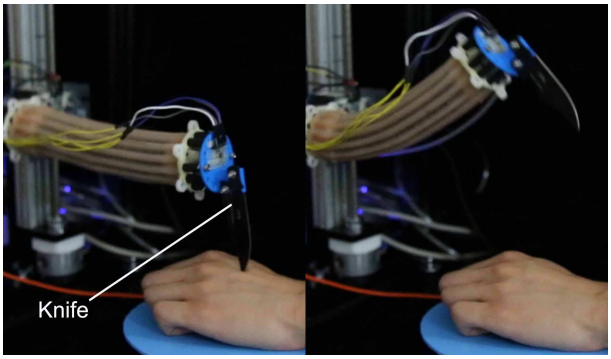


Fig. 1. IMU-based collision detection and safe reaction in dangerous human-robot interaction, with the actuator velocity of 200 mm/s. The knife did completely no harm to the volunteer.

Active stiffness tuning is an effective method to ensure flexibility and loading capacity of soft robots [8], [9]. While soft robots cannot be precisely modeled and controlled, at present realizing the variable stiffness is mainly through mechanical design [8], which can be realized by most soft pneumatic actuators, like McKibben Muscles [10], OctArm integrated with cable-actuating system [11], or TIFF-FLOP manipulator applied in minimally invasive surgery [12]. Vacuum jamming based structures are also widely used to rapidly adjust the actuator's stiffness, such as robotic arms made from granular jamming [13] and layer jamming [14]. Some contributions realize stiffness tuning using smart materials like shape memory alloys (SMAs) [15] or electroactive polymers (EAPs) [16]. However, the lightweight variable stiffness structures which could adjust stiffness rapidly and markedly are still under

Manuscript received: September, 8, 2018; Revised November, 14, 2018; Accepted January, 5, 2019.

This paper was recommended for publication by Editor P. Rocco upon evaluation of the Associate Editor and Reviewers' comments. This work was supported by the National Natural Science Foundation of China under grant 61573333 and U1613216.

[1]Nan Lin, Peichen Wu and Xiaoping Chen (corresponding author) are with the School of Computer Science and Technology, University of Science and Technology of China, Hefei, 230026, China. Correspondence to xpchen@ustc.edu.cn

[2]Fan Yang and Menghao Wang are with the School of Engineering Science and Technology, University of Science and Technology of China, Hefei, 230026, China.

[3]Jizhou Wei, Songlin Xu and Zhicheng Ye are with the School of Information Science and Technology, University of Science and Technology of China, Hefei, 230026, China.

Digital Object Identifier (DOI): see top of this page.

development.

In order to have active control, it is necessary to pair the soft actuator with tactile sensors to create a feedback control system. For soft robots, we can effectively make use of vibration characteristic of soft materials, which has already been successfully applied in haptic perception of robotic hands. For example, a three-axis force sensor is used by Beccai et al [17] to perform slip detection, and developed by de Boissieu et al. [18] to discriminate different surfaces by capturing the high-frequency vibrations that occur when rubbing a target surface. Other studies use accelerometers to detect tactile vibrations and estimate whether the object has slipped [19], which can be also applied in surface recognition and categorization [20], [21].

Inertial Measurement Units, which rely on the fusion of measurements from gyroscopes, accelerometers and a magnetometer to estimate the pose of the sensor, provide an option for both tracking robot motion and detecting vibration in three-dimensional space. But at present IMU has not been widely adopted in soft robotics. Gillespie et al. [22] use IMU to detect inflatable joint's angle, to help control both joint position and stiffness simultaneously. Yirmibesoglu et al. [23] present a microchannel strain gauge in conjunction with IMUs, to measure the bending angle of soft joint. This hybrid sensor improves the accuracy of angle measurements to some extent. But these applications are only for detecting pose in one dimension (bending angle).

This study aims to develop an active safe control strategy for variable stiffness soft robots. First we have designed a stiffness adjustable soft actuator combining pneumatic actuation, vacuum jamming and cable-driven mechanism. Using IMUs and combining piecewise constant curvature model [24], we can estimate the three-dimensional pose of the soft actuator, as well as the load weight (i.e., weight of end tools). Besides, the oscillation detected by IMUs is used for collision detection and safe reaction of soft actuators. Therefore, in contrast to rigid robots, we do not need precise models or expensive force/torque sensors to realize similar safe control effect. Experimental results further confirm that our active safe control algorithm has distinct advantages compared with passive compliance reaction of general soft robots, and human trials shown in Fig. 1 demonstrate its safety and robustness.

Our work can provide references and guidance for other soft robot researchers on active compliance control to make their robots more reliable. Meanwhile, The novel actuator can apply to anthropomorphic robot hands as dexterous fingers [25], due to its flexibility, inherent compliance and versatility of variable stiffness. Since the safe control strategy is similar to the stress response of organism, it can help sense surrounding environments during robot-environment interactions, and protect robotic hand when grasping sharp objects or bear severe shocks.

In summary, the contributions of this paper are:

1) A novel variable stiffness actuator that can maintain enough stiffness under low actuating pressure.
2) The concept of active safe control for soft robots, combining their inherent oscillation characteristics.
3) Strategies to realize load estimation, collision detection and safe reaction using low-cost IMU, which could be a general method for other continuum robots as well.

The rest of this paper is organized as follows: in Section II, we present our soft actuator, and run experiments to test its stiffness under different pressure and tendon tension. In Section III, we use neural network to estimate the load weight which has great influence on safe control of the actuator. Section IV proposes a novel method to realize active safe control. The experimental evaluation is presented in Section V, and limitations are discussed in Section VI. Finally, conclusions and future work are summarized in Section VII.

## II. VARIABLE STIFFNESS ACTUATOR

### A. Actuator Design

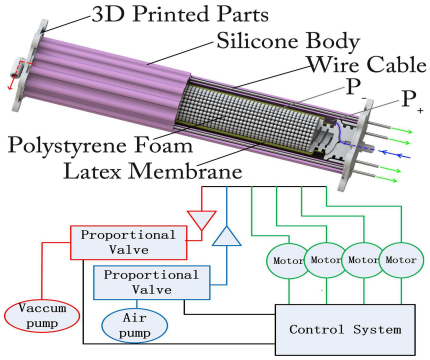


Fig. 2. Schematic of the actuator and driving system. The actuator adopts the pneumatic and tendon-driven actuation to control its motion and stiffness. Red lines represent vacuum pipes which are connected to the jamming structure. The air channels represented by blue lines control the positive pressure inside the silicone body. Tendon-driven mechanisms, represented by green lines, are mainly used for controlling the actuator's motion.

Fig. 2 shows the schematic of the actuator and driving system. Radial expansive deformation of the hollow silicone body is limited by the Kevlar fiber wounding around, so only bending and slight axial expansion are possible. Several chambers distribute uniformly on the inner edge of the silicone body. There are four steel wires traversing through the chambers and then fixed to the tip of the actuator. Inside the silicone body is a granular jamming structure filled with 1-mm diameter polystyrene foam particles. As for jamming membrane, we choose latex membrane (widely applied on soil sample analysis) with the inner diameter of 25 mm and the thickness of 0.3 mm. On the two ends of the actuator are 3D printed parts, connected to the silicone body by glue. By adjusting the displacement of steel wires, we can control the curvature and deformation direction of the actuator, similar to jammable manipulator [14] or STIFF-FLOP [12].

The external diameter of the actuator is 42 mm, and the total length is about 200 mm. With ultralight filling particles, the weight of the whole actuator is less than 70 g. Another advantage of the actuator is that it has multiple methods or structures to adjust stiffness, especially the jamming structure. Other kinds of jamming structures are actuated by vacuum pressure, which is limited by maximum negative pressure (-100 kPa Max.). But when our actuator is inflated, positive

pressures $P_+$ can not only change the stiffness of the silicone body, but also reinforce the jamming structure. Therefore, under combined actuation of positive pressure $P_+$ (outside the latex membrane) and negative pressure $P_-$ (inside the latex membrane), the jamming structure can obtain total actuating pressure $(P_+ + P_-)$. Besides, cable-driven mechanism provides additional variable stiffness ability, so even under low-pressure actuation (40 kPa), our soft actuator can still carry the load over 250 g, which is three times more than its own weight.

### B. Stiffness Test

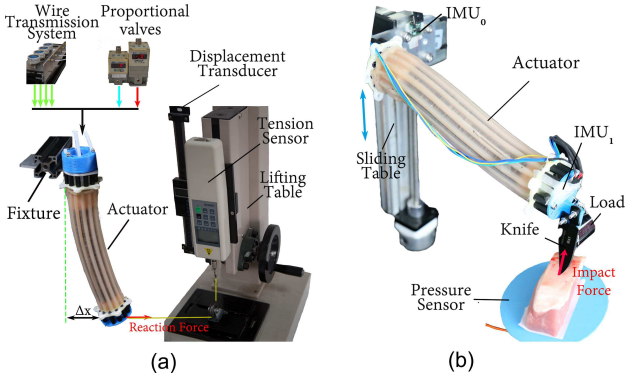


Fig. 3. The experimental platforms. (a) is used to test actuator's stiffness, while (b) is for load estimation, collision detection and safe reaction.

We have tested the characteristics of variable stiffness, Fig. 3(a) shows the experiment platform. It mainly comprises of a wire transmission system, a lifting table, a capacitive displacement transducer, and an external tension sensor. The steel wires are pulled by four precision motors (maxon, EC45 flat motor) to produce displacement. Two miniature pumps (kamoer, KVP08, $\pm$100 kPa Max.) supply the required pressure to the pneumatic proportional valve (SMC, ITV1030-012BL5, 500 kPa Max.) and the vacuum proportional valve (SMC, ITV-2090-042BS5, -80 kPa Max.) to control the internal pressure of actuator. For safety reasons, we limited positive pressure under 40 kPa and maximum negative pressure -60 kPa during the experiment.

In the stiffness test, the actuator is fixed to the base vertically, and the tension sensor is fixed to the lifting table. The tailshaft of tension sensor and the tip of actuator are connected by cable. When we adjust the displacement (measured by the displacement transducer) of the tension sensor, the actuator bends due to the pulling of cable, and the reaction force resisting this displacement change is recorded by tension sensor. Therefore, the slope of the force-displacement curve approximately represents the actuator's stiffness.

During the experiment, positive pressure $P_+$ varies from 20 kPa to 40 kPa, while negative pressure $P_-$ varies from -20 kPa to -60 kPa, and the tendon tension of cables can also be controlled (with or without tension). Experiment results are displayed in Fig. 4. From Fig. 4(a) to Fig. 4(d) are results under negative pressure of 0 kPa, -20 kPa, -40 kPa and -60 kPa, respectively. It can be seen that the stiffness is significantly

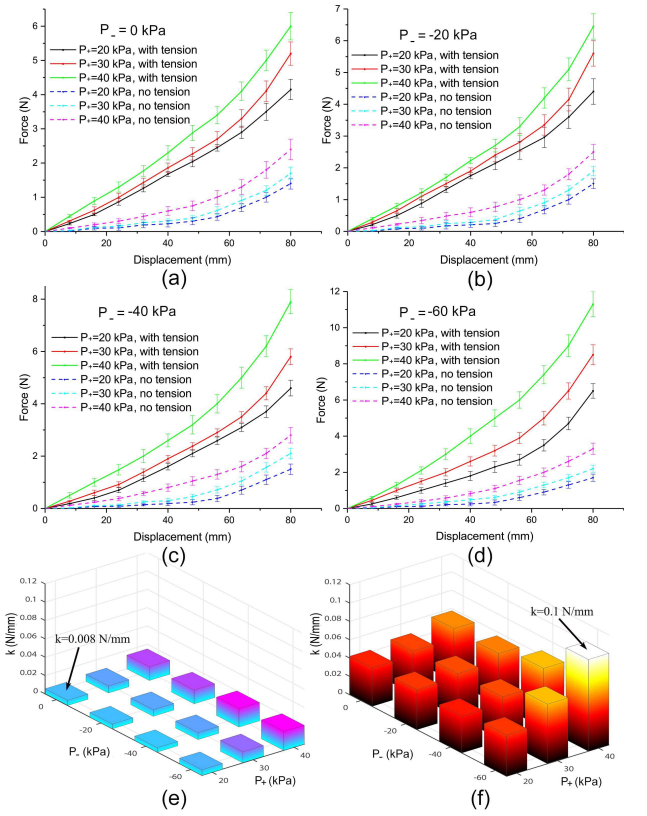


Fig. 4. Subfigures (a) to (d) demonstrate the reaction force-displacement curves under different positive pressure, negative pressure and tendon tension. The error bars show the standard deviation from the mean result obtained by pressurizing soft actuator three times. The slope approximately represents the actuator's stiffness. Subfigures (e) and (f) demonstrate the variable stiffness characteristic of the soft actuator in the linear range, where (e) and (f) represent stiffness change along with pressure without and with cable tension, respectively.

enhanced with the increase of internal pressure and tendon tension. When displacement is less than 40 mm, the relationship between pressure and displacement is approximately linear, meaning that the stiffness $k$ is almost constant. When displacement exceeds 40 mm, the actuator's stiffness increases rapidly. This is mainly caused by the non-ideal deformation of silicone body. Besides, in the linear range, the maximum stiffness is more than ten times of the minimum stiffness, so under allowable load (less than 150 g), the actuator is able to maintain its arc shape, which can be applied to subsequent collision detection.

## III. LOAD ESTIMATION

The actuator has relatively small stiffness, so end-load will have great effect on its motion and collision detection. Therefore we must calibrate the weight of the end-load first for the following modeling and control. Here we simply assume the end-load is a mass point, ignoring its shape. Although the dynamic model of cable-driven continuum robots can be built [26], it remains to be tested and have several limitations in practical applications. Here we choose a simple neural network to estimate the load instead of precise model. Experimental setup is shown in Fig. 3(b). Two IMUs, whose Z-axes are

vertical to the mounting surface, are fixed to the both ends of the actuator to measure the orientation of the tip frame in the base frame. Before estimating loads, the actuator is adjusted to its zero position (displacement of all cables equals to initial length). When the load is mounted, the actuator is bent and the tip frame deviates from its initial pose. We take the angle between Z-axes of the base frame and the present tip frame as an input ($Angle_Z$). The other inputs are positive pressure $P_+$ and negative pressure $P_-$, because they can regulate the internal pressure rapidly and accurately to change actuator's stiffness, thus influence the pose of tip frame. The cable tension is not used here to adjust stiffness, because limited by manufacturing technology, there will be uncontrollable friction and displacement between cables and silicone chambers, bringing in large errors.

The neural network is composed of an input layer, two dense layers (16 nodes for each) and an output layer, the output of neural network is the load weight $m_l$. More specifically, to avoid the range of input data affecting the training effect, we normalize the input data using the Z-score normalization method at first. And a $ReLU$ nonlinear activation function is used after each dense Layer to achieve better fitting ability.

3000 sets of raw data are generated for training. Testing weights range from 50 g to 250 g. Its accuracy is tested using 400 random target objects (pre-weighted by analytical balance with 0.1 g accuracy). Fig. 5 (a) shows the difference between the predicted value and the actual value and Fig. 5 (b) shows the distribution of relative error. Finally, we get the average relative error of 8.25%. However, because of the soft structure's viscoelasticity and IMUs' accidental abnormal values affected by outside magnetic interference, sometimes the relative error would still reach over 40%, which can not be eliminated in single measurement

Thanks to the variable stiffness characteristic, we can run multiple tests to further decrease error and eliminate these abnormal values. In the experiment, we change the actuator's internal positive and negative pressure 7 times to adjust its stiffness online. For every status with different stiffness, we estimate a load weight with the neural network. The largest and smallest results are discarded and the mean of the remaining 5 values (i.e. truncated mean) is computed as estimated load weight. Finally the average relative error reduces to 6.2%, and abnormal values do not show up again in the existing experimental results, which is acceptable for soft robots [27].

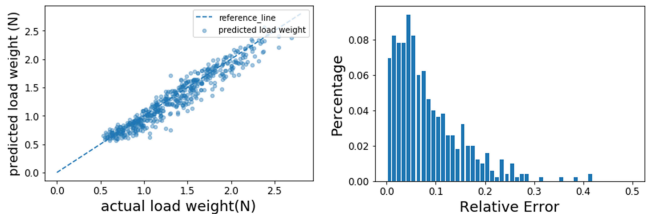


(a) (b)

Fig. 5. The accuracy of load estimation. In subfigure (a), the X-axis and Y-axis represent the actual value and prediction value of load weights respectively. (b) demonstrates the distribution of relative error.

## IV. COLLISION DETECTION AND SAFE REACTION

### A. Simplified Model

A kinematic model should be established to obtain the relationship between the actuator's motion (task space) and the wire's displacement (actuation space). Here the pressures are not taken as actuation variables, for they only have an influence on actuator's stiffness, but no effect on the kinematic model. Because real-time computing is required for collision detection and safe reaction, it is impossible to solve it by means of finite element analysis. We adopt the simplified model that widely applied in continuum robots, the Piecewise Constant Curvature (PCC) model [24], as shown in Fig. 6(a) and (b). In this model, the actuator is simplified to a spatial arc through its axis. The curve consists of triplets of bending angle $\theta$, the angle of the plane containing the arc $\phi$ and arc length $l$, called the parameters of configuration space. Two coordinates are established at both ends of the curve model, in which the Z-axis of the coordinate system is tangent to the curve. The transformations between three spaces have analytical solutions [24]. Especially, the mapping $f_{independent}$ from configuration space to task space is robot–independent, which ensures that our algorithm can be applied to other continuum robots. The shortcoming of this model is that it does not take into account the influence of gravity and dynamics, which would bring in certain errors.

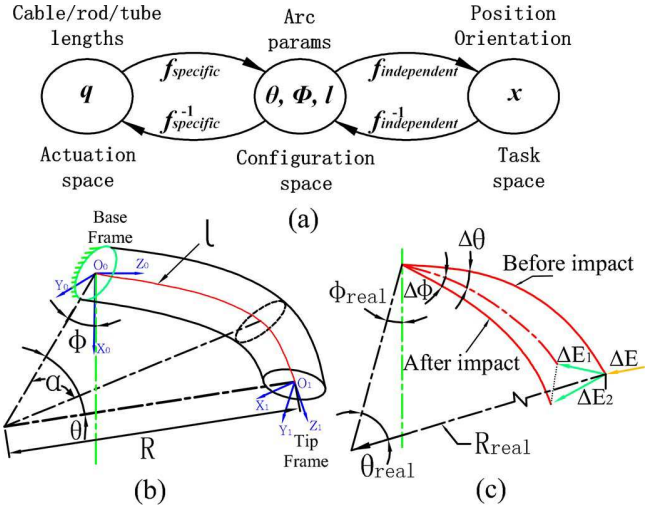


Fig. 6. (a) Two-level kinematic model architecture. Controlled variable are separated into three spaces. The mapping $f_{specific}$ from actuation space $q$ to the configuration space of arc parameters is robot-specific, and the mapping $f_{independent}$ from arc parameters to pose $x$ along the backbone is robot-independent. (b) The sketch of continuum robot's Piecewise Constant Curvature model, where the configuration space parameters, base frame and tip frame are demonstrated. Green dashed line represents the reference line of the initial state ($\phi = 0$). (c) The simplified impact model of the actuator. The red dot-dash line represents the actuator's equivalent curve projected in the $\phi$-plane.

### B. Model-Based Collision Detection

During the motion process of soft actuators or manipulators, when they collide with environment or human body, the impact will cause the oscillation of soft structures. The vibration amplitude decays rapidly because of system damping.

The control algorithm detects this vibration in real time, if the amplitude exceeds a certain threshold, the collision is considered to have happened, then the corresponding safe reaction will be taken. However in reality, the low-cost IMU is generally only used for pose estimation, not suitable for detecting absolute displacement (would cause large cumulative error). Therefore we indirectly estimate the direction of the oscillation by combining pose estimation with PCC model. Besides, the actuator's normal movement will interfere with the collision detection, which should be compensated for.

Firstly, we calculate actuator's pose in the base frame. Suppose under world coordinate system, the rotation transformation matrixes (obtained directly through IMUs) of $IMU_0$ and $IMU_1$ are ${}^0R_{world}$ and ${}^1R_{world}$, respectively. Then transformation ${}^1R_0$ from base frame to tip frame is:

$$ {}^1R_0 = {}^1R_{world}\left({}^0R_{world}\right)^{-1} = R \triangleq \begin{bmatrix} \boldsymbol{n} & \boldsymbol{o} & \boldsymbol{a} \end{bmatrix} \tag{1} $$

Where $R$ is the rotation transformation matrix part of $f_{independent}$ mapping, and the corresponding expression can be found in [24].

Because IMU cannot detect absolute displacement, we are unable to directly obtain the arc length. Since the actuator can only elongate slightly, we take the average length of steel wires to approximately represent the actuator's arc length. The bending angle $\theta_{real}$, rotation angle $\phi_{real}$ and the actuator's arc length $l$ of the IMU-estimated model are calculated as:

$$ \begin{cases} \theta_{real} = \cos^{-1}(a_z) \\ \phi_{real} = \tan^{-1}(\dfrac{a_y}{a_x}) \\ l = min\{\dfrac{\sum_{i=1}^{4} l_i}{4}, l_{max}\} \end{cases} \tag{2} $$

Where $\boldsymbol{a} = \begin{bmatrix} \boldsymbol{a_x} & \boldsymbol{a_y} & \boldsymbol{a_z} \end{bmatrix}^T$ is the third column of rotation transformation matrix $R$. $l_i (i = 1...4)$ is the displacement of four steel wires, and $l_{max}$ is the allowable maximum arc length. As for other extensible actuators, extra displacement sensors might be needed. Note that when we control the actuator's motions, we can only adjust the configuration space parameters $\theta_{ideal}, \phi_{ideal}, l_{ideal}$ by controlling variables in actuator space (i.e. displacements of steel wires). There would be deviations between these parameters and the estimated result of IMUs (mainly affected by gravity), but the method still works under certain loads.

In order to eliminate the influence on collision detection caused by the actuator's normal movement, we define impact variables $\Delta\theta$ and $\Delta\phi$ to represent the variation of configuration-space parameters during the interval $\Delta t$.

$$ \begin{cases} \Delta\theta = \Delta\theta_{real} - \Delta\theta_{ideal} \\ \Delta\phi = \Delta\phi_{real} - \Delta\phi_{ideal} \end{cases} \tag{3} $$

Where $\Delta\theta_{real}$, $\Delta\phi_{real}$ and $\Delta\theta_{ideal}$, $\Delta\phi_{ideal}$ are variations estimated by IMUs and variations of the actuator's normal motion in configuration space, respectively.

Next we estimate impact energy via the simplified impact model. The actuator is assumed to be a uniform elastomer that conforms to the PCC model, regardless of the gravity influence in normal motion. When impact happens, the impact energy transforms into load's gravitational potential energy and actuator's elastic potential energy. The actuator is lightweight, and the average displacement after the impact is small enough compared with end-load, so the actuator's own gravitational potential energy change is just ignored.

The actuator's impact model is highly nonlinear without exact analytical solution, in order to obtain an approximate solution, the impact is simply divided into components $\Delta E_1$ in $\phi_{real}$ plane and $\Delta E_2$ vertical to $\phi_{real}$ plane, which we suppose will not have motion coupling, as shown in Fig. 6.

The impact component in $\phi_{real}$ plane $\Delta E_1$ is expressed as:

$$ \Delta E_1 = m_l g \Delta h_1 + \Delta V_{\varepsilon 1} \tag{4} $$

Where $m_l$ is load weight estimated by the neural network, $g$ is gravitational acceleration, $\Delta h_1$ is the variation of load's barycenter in height, and $\Delta V_{\varepsilon 1}$ is the variation of the actuator's elastic potential energy in $\phi_{real}$ plane. Suppose the bending moment $M_1$ is constant in each random cross section of the actuator, then the strain energy $V_{\varepsilon 1}$ is calculated as:

$$ V_{\varepsilon 1}(\theta) = \frac{M_1^2 l}{2EI} = \frac{EI\theta^2}{2l} \tag{5} $$

Where $E$ is elastic modulus, $I$ is area moment of inertia, and $l$ is the actuator's arc length. $\Delta V_{\varepsilon 1}$ is calculated as:

$$ \Delta V_{\varepsilon 1} = V_{\varepsilon 1}(\theta_{real} + \Delta\theta) - V_{\varepsilon 1}(\theta_{real}) \tag{6} $$

According to geometric relationship, $\Delta h_1$ can be approximately written as:

$$ \begin{aligned} \Delta h_1 = \{ & \frac{l}{\theta_{real} + \Delta\theta} \cos(\theta_{real} + \Delta\theta) - \frac{l}{\theta_{real} + \Delta\theta} \\ & - (\frac{l}{\theta_{real}} \cos\theta_{real} - \frac{l}{\theta_{real}}) \} \cos\phi \end{aligned} \tag{7} $$

Similarly, the vertical impact energy $\Delta E_2$ is:

$$ \Delta E_2 = m_l g \Delta h_2 + \Delta V_{\varepsilon 2} \tag{8} $$

With regard to the impact component vertical to $\phi_{real}$ plane, we assume that there is a constant contact force $F$ which causes the actuator's bending and twisting. $\alpha$ is the bending angle of a random cross section, as shown in Fig. 6. $G$ is shear modulus, $R_{real} = \frac{l}{\theta_{real}}$ is the IMU-estimated curvature radius. Bending moment $M_2$ and twisting moment $T_2$ are expressed as follows:

$$ \begin{cases} M_2 = F R_{real} \sin\alpha \\ T_2 = F R_{real}(1 - \cos\alpha) \end{cases} \tag{9} $$

The vertical impact model, which couples bending with twisting, is troublesome to deal with. Considering the actuator's cross section size is smaller than its curvature radius $R_{real}$, we simply adopt the strain energy equation of a straight bar, where

$$ V_{\varepsilon 2} = \int_0^{\theta} dV_{\varepsilon 2} = \int_0^{\theta} \frac{M_2^2 R_{real}}{2EI} + \frac{T_2^2 R_{real}}{2GI_p} d\alpha \tag{10} $$

Then the change of strain energy $\Delta V_{\varepsilon 2}$ is expressed as:

$$ \begin{aligned} \Delta V_{\varepsilon 2} = & V_{\varepsilon 2}(\theta_{real} + \Delta\theta, \phi_{real} + \Delta\phi, R_{real} + \Delta R) \\ & - V_{\varepsilon 2}(\theta_{real}, \phi_{real}, R_{real}) \end{aligned} \tag{11} $$

The angle $\Delta\phi$, which is mainly generated by twisting moment $T_2$, can be calculated as the integral of the twist angle:

$$\begin{aligned}\Delta\phi &= \int_0^l \frac{T_2 dL}{GI_p} = \frac{FR_{real}^2(\theta_{real} - \sin\theta_{real})}{GI_p} \\ \Rightarrow F &= \frac{GI_p\Delta\phi}{R_{real}^2(\theta_{real} - \sin\theta_{real})}\end{aligned} \tag{12}$$

And the displacement generated by vertical impact component can be approximately calculated as the deflection $\delta$, then the variation of the load's barycenter $\Delta h_2$ in height is written as:

$$\Delta h_2 = \delta \sin\phi_{real} = \frac{V_{\varepsilon 2}(\theta_{real}, \phi_{real}, R_{real})}{F}\sin\phi_{real} \tag{13}$$

Finally, if $\Delta E = \Delta E_1 + \Delta E_2$ exceeds the constant threshold $[\sigma_{high}]$, collision is considered to have happened. Since there are relatively large errors in manufacturing technology of soft robotics, the threshold $[\sigma_{high}]$ needs to be adjusted manually for our soft actuator at present to acquire the best performance, but the safe control strategy is universal for other tasks.

### C. Reaction Strategy

Once the collision is detected, safe reactions should be taken. The simplest safe reaction is to stop the robot as soon as possible. This may not be able to eliminate the interference with the environment. Another strategy is making the actuator move rapidly in the direction of impact force, away from the impact point. Suppose at the moment of collision (before safe reaction), $\theta_{real}^{'}$ and $\phi_{real}^{'}$ are parameters estimated by IMUs, $\Delta\theta^{'}$ and $\Delta\phi^{'}$ are the variations detected. After the safe reaction, the actuator should keep farther away from the impact point than the position of maximum oscillation amplitude:

$$\begin{cases} |\delta_1| = \left|\theta_{real} - \theta_{real}^{'} - \Delta\theta^{'} - K\dfrac{\Delta E}{m}\right| \le [\delta_1] \\ |\delta_2| = \left|\phi_{real} - \phi_{real}^{'} - \Delta\phi^{'} - K\dfrac{\Delta E}{m}\right| \le [\delta_2] \end{cases} \tag{14}$$

Where $\theta_{real}$ and $\phi_{real}$ are real-time configuration space parameters estimated by IMUs during safe reaction. $\delta_1$ and $\delta_2$ are real-time error. $[\delta_1]$ and $[\delta_2]$ are the allowable error. Meanwhile, the impact strength and load weight also affect safe reactions. The actuator is expected to go further away from impact point when facing larger impacts, and under heavier load, its motion range gets smaller, which is involved in $\frac{K\Delta E}{m}$.

But actually what we could control are the configuration space parameters $\theta_{ideal}$ and $\phi_{ideal}$. Here a simple feedback control strategy is adopted.

$$\begin{cases} \theta_{ideal}(t) = \theta_{ideal}(t-1) + K_1\delta_1(t-1) \\ \phi_{ideal}(t) = \phi_{ideal}(t-1) + K_2\delta_2(t-1) \end{cases} \tag{15}$$

After safe reaction and a two-second delay, we continue detecting the impact strength. If it is still larger than $[\sigma_{low}]$ (the value is also manually adjusted to ensure satisfying performances and guarantee the actuator can eventually return to zero position), then safe control continues, otherwise the actuator slowly returns to its zero position.

During the safe reaction, the actuator's stiffness also can be tuned to reduce the impact. When the collision is detected, the actuator's stiffness is adjusted to be low immediately. In subsequent safe reactions, stiffness gradually increases until the actuator reaches safe position. This can also reduce impact damage to a certain extent. The whole process of reaction strategy is demonstrated in Fig. 7.

Finally, compliance control can be considered as a special case of collision detection and safe reaction, where $[\sigma_{high}] \approx 0$. Thus we can realize similar lead-through programming functionality of rigid manipulators.

## V. EXPERIMENTS WITH THE VARIABLE STIFFNESS ACTUATOR

The experiment equipment for collision detection is shown in Fig. 3(b). The actuator is mounted on the electric slide, which is able to move upwards and downwards at a given velocity. A pressure sensor (freud, DHMH-106, 1% F.S., 1kg Max) is used to measure the impact force, and the 3-axis angular velocity and angle are measured by IMUs (MPU-9250, $0.1^\circ$ measuring accuracy), with the highest acquisition frequency of 200 Hz.

In the experiment, a piece of pork (similar to human-body tissues) is placed on the pressure sensor. A sharp knife and a variable weight load are fixed to the tip of the actuator. When the actuator bends or moves downwards, if the knife collides with the pork, contact force can be obtained immediately by high-precision pressure sensor. To verify the effectiveness of our algorithm, four collision detection and safe reaction strategies are defined, as listed below.

- **Keep moving without any reaction (Strategy 0)**
  This strategy is the passive compliance reaction of soft actuators.
- **Emergency stop (Strategy 1)** This strategy uses model-based collision detection, and stops the rectilinear or bending motions as soon as a collision is detected.
- **Angular velocity based detection and reaction (Strategy 2)**
  This strategy takes the data of 3-axis angular velocity (measured directly by the IMUs) and the estimated load weight as input. If $m_l(\omega^2(t+\Delta t) - \omega^2(t)) \ge [D]$, where

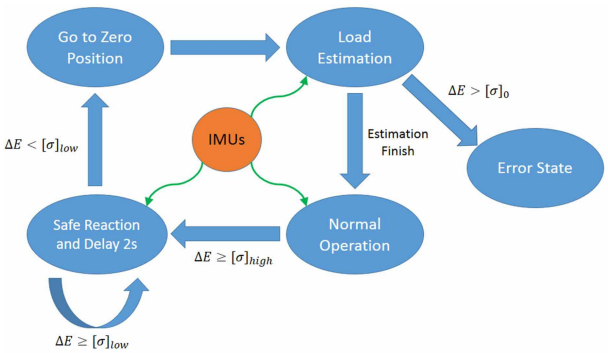


Fig. 7. Soft actuator operation states.

$[D]$ is a constant threshold, collision is considered to have happened. The actuator moves away from the impact point using aforementioned reaction method.

- **Model-based detection and reaction (Strategy 3)** This strategy uses the model-based collision detection and safe reaction method described above.

During the experiment, total 50 g or 150 g load is fixed to the tip of the actuator. The normal motion of soft actuator is controlled by tendon-driven system. In one set of experiments, the actuator holds its initial state (horizontal), and vertical velocity $v$ is 50 mm/s or 240 mm/s. In the other set, the slide remains upright and stationary, the actuator bends at constant angular velocities $\omega$ 0.3 rad/s or 0.8 rad/s. Experiment results are shown in Fig. 8, (a) and (b) demonstrate the contact force in rectilinear motions, while (c) and (d) are bending motions. When the actuator keeps moving without any collision detection (Strategy 0), the impact force of the soft actuator is significantly larger than that of other three strategies. Therefore, when end load is larger than 150 g, even at the velocity of 50 mm/s, the impact force would still make the knife stab into the pork, causing severe damage to biological tissue. This demonstrates that passive compliance is not able to guarantee safety in dangerous environments.

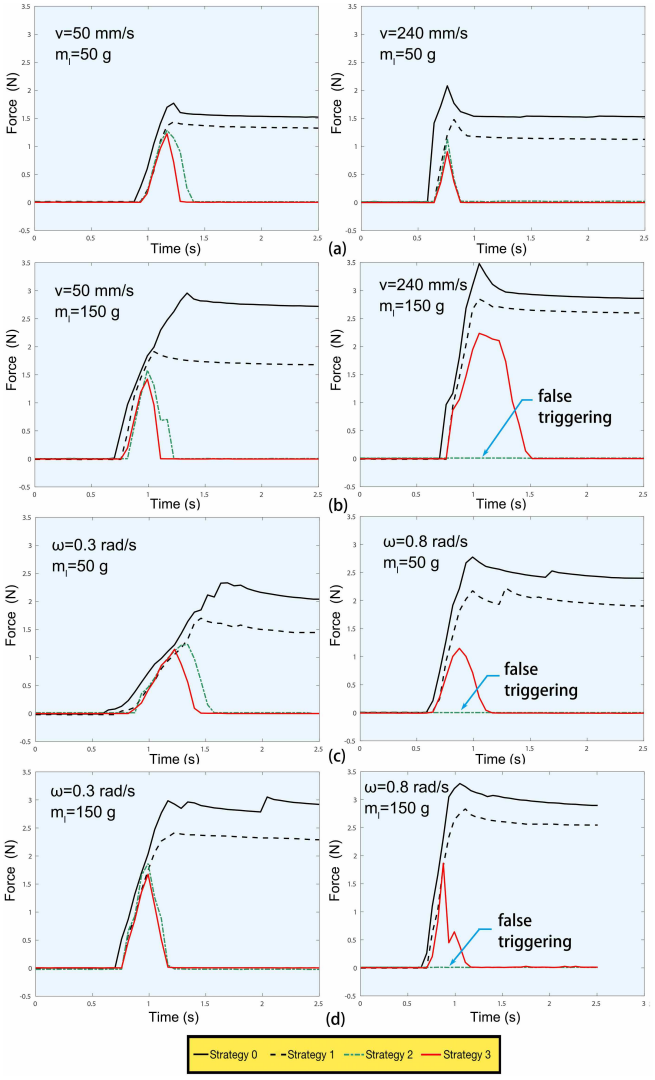


Fig. 8. Experimental results of collision detection and safe reaction with different velocities, load weights and motion types. (a) and (b) demonstrate the contact force in rectilinear motions, while (c) and (d) are the results of bending motions. Four control strategies are tested and compared.

Under low velocity and light load, the performance of Strategy 1 is acceptable, for model-based collision detection can detect the impact rapidly, and urgently stop the actuator. However under high velocity and heavy load, Strategy 1 will generate large impact force. Even if the motion stops immediately, the actuator is still in the oscillation state, which would generate additional impact to biological tissue. Besides, the impact force of Strategy 1 would not decrease, which means the knife would remain contact with biological tissue, causing serious safety hazards.

Strategy 2 performs similarly to Strategy 3 in rectilinear motion with light load. The contact force with the object quickly turns to zero after the reaction. But the performance under heavy load is less satisfying. This is mainly because when impact occurs under heavy load, the actuator's oscillation is not obvious enough (same for Strategy 3). The most severe problem of Strategy 2 is that it did not compensate for the actuator's own normal motions. Therefore when the actuator makes rapid bending motion, its normal motion would cause variation of angular velocity, thus lead to false triggering. This phenomenon also appears multiple times in rectilinear motions with heavy load and high velocity. This circumstance is even worse if the actuator has a certain acceleration.

Strategy 3 performs best among all the strategies. Its performance under high velocity is roughly the same as that under low velocity. This is because although there is larger momentum under high velocity, the oscillation is also more obvious when impact occurs, hence the collision will be detected earlier and reaction be taken more quickly. So even under high velocity and heavy load, we can still detect collision and take corresponding safe reaction in time. The maximum impact force is no larger than 2.5 N, which creates the least damage to biological tissue.

## VI. DISCUSSION

Our strategy successfully settles the problem of collision detection and safe reaction for a single actuator. However, there are still several limitations.

- Load estimation at any position. At present the neural network based method can only calibrate load weight at the zero position. In order to calibrate load weight at any position, more data needs to be collected for enhanced neural networks, or the model-based method may be considered.
- The influences of dynamics are not taken into account and there are too many simplifications. Once the actuator operates at high speed or acceleration, some factors like inertia force cannot be ignored anymore, because even its own motion could cause obvious oscillations. The actuator's gravity that is disregarded in the PCC model and simplifications in the impact model will also result in unacceptable error in some cases. Therefore more

precise model needs to be established in the next step, and manufacture technique should be improved.

- How our strategy can be applied to multi-segment continuum robots. Multi-segment continuum robots use more than three IMUs, so we must adopt multi-sensor data fusion technology for pose estimation and safe reaction. Meanwhile, the couplings of motion severely influence the control effect, which could be solved by combining other measurement devices like 3D vision sensor.

## VII. CONCLUSION AND FUTURE WORK

In this paper, we proposed a variable stiffness actuator which integrates pneumatic actuation, vacuum jamming and tendon driving. The actuator's tunable stiffness structure makes it flexible and lightweight enough to adapt to unstructed environments while maintaining its load capability. IMU-based load estimation, collision detection and safe reaction strategies are presented, combining the variable stiffness and inherent compliance characteristics of the actuator. The effectiveness of our strategy is verified through experiment, compared with other three strategies. We also carried out the experiment on human body, the safety still can be guaranteed at speeds of up to 200 mm/s using our algorithm.

The highlights of our control strategy lie on that we accomplish a series of calibration and control tasks only using the low-cost IMUs, and achieve similar control effects as sophisticated rigid robots. Meanwhile, our algorithm is universal, which means that it can be applied to other continuum or soft robots as well. In the future, collision detection and reaction strategies of multi-segment continuum robots will be considered, and the models will be further improved to obtain better control effects. The accompanying video provides a demonstration of the proposed actuator and control strategies.

## REFERENCES


[1] S. Kim, C. Laschi, and B. Trimmer, "Soft robotics: a bioinspired evolution in robotics," *Trends in biotechnology*, vol. 31, no. 5, pp. 287–294, 2013.

[2] N. Kellaris, V. G. Venkata, G. M. Smith, S. K. Mitchell, and C. Keplinger, "Peano-hasel actuators: Muscle-mimetic, electrohydraulic transducers that linearly contract on activation," *Science Robotics*, vol. 3, no. 14, p. eaar3276, 2018.

[3] D. Rus and M. T. Tolley, "Design, fabrication and control of soft robots," *Nature*, vol. 521, no. 7553, p. 467, 2015.

[4] S. Haddadin, A. Albu-Schaffer, A. De Luca, and G. Hirzinger, "Collision detection and reaction: A contribution to safe physical human-robot interaction," in *Intelligent Robots and Systems, 2008. IROS 2008. IEEE/RSJ International Conference on*. IEEE, 2008, pp. 3356–3363.

[5] S. Haddadin, A. Albu-Schäffer, and G. Hirzinger, "Soft-tissue injury in robotics," in *Robotics and Automation (ICRA), 2010 IEEE International Conference on*. IEEE, 2010, pp. 3426–3433.

[6] H. Jiang, Z. Wang, X. Liu, X. Chen, Y. Jin, X. You, and X. Chen, "A two-level approach for solving the inverse kinematics of an extensible soft arm considering viscoelastic behavior," in *Robotics and Automation (ICRA), 2017 IEEE International Conference on*. IEEE, 2017, pp. 6127–6133.

[7] Y. Jin, Y. Wang, X. Chen, Z. Wang, X. Liu, H. Jiang, and X. Chen, "Model-less feedback control for soft manipulators," in *Intelligent Robots and Systems (IROS), 2017 IEEE/RSJ International Conference on*. IEEE, 2017, pp. 2916–2922.

[8] M. Manti, V. Cacucciolo, and M. Cianchetti, "Stiffening in soft robotics: a review of the state of the art," *IEEE Robotics & Automation Magazine*, vol. 23, no. 3, pp. 93–106, 2016.

[9] Y. Yang, Y. Chen, Y. Li, M. Z. Chen, and Y. Wei, "Bioinspired robotic fingers based on pneumatic actuator and 3d printing of smart material," *Soft robotics*, vol. 4, no. 2, pp. 147–162, 2017.

[10] M. E. Giannaccini, C. Xiang, A. Atyabi, T. Theodoridis, S. Nefti-Meziani, and S. Davis, "Novel design of a soft lightweight pneumatic continuum robot arm with decoupled variable stiffness and positioning," *Soft robotics*, vol. 5, no. 1, pp. 54–70, 2018.

[11] W. McMahan, V. Chitrakaran, M. Csencsits, D. Dawson, I. D. Walker, B. A. Jones, M. Pritts, D. Dienno, M. Grissom, and C. D. Rahn, "Field trials and testing of the octarm continuum manipulator," in *Robotics and Automation, 2006. ICRA 2006. Proceedings 2006 IEEE International Conference on*. IEEE, 2006, pp. 2336–2341.

[12] A. Shiva, A. Stilli, Y. Noh, A. Faragasso, I. De Falco, G. Gerboni, M. Cianchetti, A. Menciassi, K. Althoefer, and H. A. Wurdemann, "Tendon-based stiffening for a pneumatically actuated soft manipulator," *IEEE Robotics and Automation Letters*, vol. 1, no. 2, pp. 632–637, 2016.

[13] N. G. Cheng, M. B. Lobovsky, S. J. Keating, A. M. Setapen, K. I. Gero, A. E. Hosoi, and K. D. Iagnemma, "Design and analysis of a robust, low-cost, highly articulated manipulator enabled by jamming of granular media," in *Robotics and Automation (ICRA), 2012 IEEE International Conference on*. IEEE, 2012, pp. 4328–4333.

[14] Y.-J. Kim, S. Cheng, S. Kim, and K. Iagnemma, "Design of a tubular snake-like manipulator with stiffening capability by layer jamming," in *Intelligent Robots and Systems (IROS), 2012 IEEE/RSJ International Conference on*. IEEE, 2012, pp. 4251–4256.

[15] C. Laschi, M. Cianchetti, B. Mazzolai, L. Margheri, M. Follador, and P. Dario, "Soft robot arm inspired by the octopus," *Advanced Robotics*, vol. 26, no. 7, pp. 709–727, 2012.

[16] M. Henke, J. Sorber, and G. Gerlach, "Multi-layer beam with variable stiffness based on electroactive polymers," in *Electroactive Polymer Actuators and Devices (EAPAD) 2012*, vol. 8340. International Society for Optics and Photonics, 2012, p. 83401P.

[17] L. Beccai, S. Roccella, A. Arena, F. Valvo, P. Valdastri, A. Menciassi, M. C. Carrozza, and P. Dario, "Design and fabrication of a hybrid silicon three-axial force sensor for biomechanical applications," *Sensors and Actuators A: Physical*, vol. 120, no. 2, pp. 370–382, 2005.

[18] F. De Boissieu, C. Godin, B. Guilhamat, D. David, C. Serviere, and D. Baudois, "Tactile texture recognition with a 3-axial force mems integrated artificial finger." in *Robotics: Science and Systems*. Seattle, WA, 2009, pp. 49–56.

[19] R. D. Howe and M. R. Cutkosky, "Sensing skin acceleration for slip and texture perception," in *Robotics and Automation, 1989. Proceedings., 1989 IEEE International Conference on*. IEEE, 1989, pp. 145–150.

[20] V. Sukhoy, R. Sahai, J. Sinapov, and A. Stoytchev, "Vibrotactile recognition of surface textures by a humanoid robot," in *IEEE International Conference on Robotics and Automation*, vol. 1, 1989, pp. 145–150.

[21] J. Sinapov, V. Sukhoy, R. Sahai, and A. Stoytchev, "Vibrotactile recognition and categorization of surfaces by a humanoid robot," *IEEE Transactions on Robotics*, vol. 27, no. 3, pp. 488–497, 2011.

[22] M. T. Gillespie, C. M. Best, and M. D. Killpack, "Simultaneous position and stiffness control for an inflatable soft robot," in *Robotics and Automation (ICRA), 2016 IEEE International Conference on*. IEEE, 2016, pp. 1095–1101.

[23] O. D. Yirmibesoglu and Y. Menguc, "Hybrid soft sensor with embedded imus to measure motion," in *Automation Science and Engineering (CASE), 2016 IEEE International Conference on*. IEEE, 2016, pp. 798–804.

[24] R. J. Webster III and B. A. Jones, "Design and kinematic modeling of constant curvature continuum robots: A review," *The International Journal of Robotics Research*, vol. 29, no. 13, pp. 1661–1683, 2010.

[25] R. Deimel and O. Brock, "A novel type of compliant and underactuated robotic hand for dexterous grasping," *The International Journal of Robotics Research*, vol. 35, no. 1-3, pp. 161–185, 2016.

[26] F. Renda, M. Giorelli, M. Calisti, M. Cianchetti, and C. Laschi, "Dynamic model of a multibending soft robot arm driven by cables," *IEEE Transactions on Robotics*, vol. 30, no. 5, pp. 1109–1122, 2014.

[27] C. S. Kothera, M. Jangid, J. Sirohi, and N. M. Wereley, "Experimental characterization and static modeling of mckibben actuators," *Journal of Mechanical Design*, vol. 131, no. 9, p. 091010, 2009.